



ELSEVIER

Available online at www.sciencedirect.com

ScienceDirect

journal homepage: www.elsevier.com/locate/ijhe

Controlling hydrogen evolution on iron electrodes

Jorge Omar Gil Posada*, Peter J. Hall

Chemical and Biological Engineering, University of Sheffield, Sir Robert Hadfield Building, Mapping Street, Sheffield S1 3JD, England, UK

ARTICLE INFO

Article history:

Received 24 February 2016

Accepted 10 April 2016

Available online xxx

Keywords:

Iron electrode

NiFe

Electrolyte decomposition

Cell performance

Hydrogen evolution

ABSTRACT

Aiming to develop a cost effective means to store large amounts of electric energy, NiFe batteries were produced and tested under galvanostatic conditions at room temperature. Multiple regression analysis was conducted to develop predictive equations that establish a link between hydrogen evolution and electrode manufacturing conditions, over a wide range of electrode/electrolyte systems. Basically, the intent was to investigate the incidence of lithium hydroxide and potassium sulphide as electrolyte additives on cell performance. With this in mind, in-house built Fe/FeS based electrodes were cycled against commercially available nickel electrodes on a three electrode cell configuration. A 3×4 full factorial experimental design was proposed to investigate the combined effect of the aforementioned electrolyte additives on cell performance. As a consequence, data from 144 cells were finally used in conducting the analysis and finding the form of the predictive equations. Our findings suggest that at the level of confidence $\alpha = 0.05$, the presence of relatively large amounts of the soluble bisulphide would enhance the performance of the battery by reducing electrolyte decomposition.

© 2016 The Authors. Published by Elsevier Ltd on behalf of Hydrogen Energy Publications LLC. This is an open access article under the CC BY license (<http://creativecommons.org/licenses/by/4.0/>).

Introduction

Fossil fuels are, by definition, non-renewable energy sources that have fulfilled our energy needs during modern times. However, if we keep using them non-stop as before, in the long run, we will, inevitably, exhaust our planetary resources, for they can't be replenished (or at least, it would be impractical). Renewable sources, on the other way, have the potential to provide large amounts of energy without exhausting them. It is imperative to find cost effective ways to store energy coming from these sources [1]. The knowledge of these aspects has prompted an increasing demand of energy from renewable sources [2–7].

Unfortunately, the availability of renewable sources (such as temporary energy profiles, availability of sun light, sufficient

supply of water, etc.) has restricted their use. In essence, the natural incompatibility between energy generation and demand must be addressed otherwise a large scale utilization of renewable sources would be unviable. Moreover, the use of renewable sources such as wind or solar would produce electricity, which is not easy to store, while reducing carbon dioxide production [8,9]. Basically the best way to store electricity is to convert electricity into a non-electric form of energy (chemical, kinetic, potential, etc.), once electricity is needed, the non-electric form of energy is reverted back into electricity for further use. Basically, sustainable energy storage has been identified as a global challenge that requires solution [6,10].

Nickel-iron cells are secondary batteries that were successfully commercialized back in the early 20th century but fell out of favour with the advent of cheaper lead acid

* Corresponding author. Tel.: +44 (0)1142228257; fax: +44 (0)1142227501.

E-mail address: j.o.gil-posada@sheffield.ac.uk (J.O.G. Posada).

<http://dx.doi.org/10.1016/j.ijhydene.2016.04.123>

0360-3199/© 2016 The Authors. Published by Elsevier Ltd on behalf of Hydrogen Energy Publications LLC. This is an open access article under the CC BY license (<http://creativecommons.org/licenses/by/4.0/>).

batteries. There are many reasons favouring the use of NiFe cells as cost effective solutions to store grid-scale amounts of energy, such as: low cost of raw materials, environmentally friendliness, tolerance to electrical abuse, long life (in the order of thousands cycles of charge and discharge) and compatibility with PV's [11]. Moreover, it has been recognized that this technology would be suitable for relatively low specific energy applications ($30\text{--}50\text{ W h kg}^{-1}$) [12]. As a consequence, there are good reasons to foresee a large scale utilization of this technology; but there is a plethora of challenges to overcome first, such as increasing the cell efficiency, preventing electrolyte decomposition and therefore the evolution of hydrogen, and increasing energy and power densities [13,14].

One of the reasons for the attractiveness of NiFe cells is related with the abundance of the raw materials required for their construction. Iron is not only relatively easy to shape into different forms, but it is also the fourth most abundant element in the Earth's crust; the liquid core of our home planet is thought to be mainly composed of iron [15,16]. Although, less abundant, nickel is believed to be the second most abundant element in the Earth's core; in addition, large deposits of nickel ore can be found in many countries including Brazil, Russia, Philippines, Canada, Australia, Indonesia, etc. [17,18]. Even less abundant than nickel, bismuth is considered the 64th most abundant element in the Earth's crust [19,20], but only small amounts of this element are required in the production of iron electrodes. So a shortage of any of the aforementioned elements is not going to take place any time soon. Unfortunately, the process of extraction of metals such as iron renders huge amounts of carbon dioxide [21]. Recyclability of battery components, as with lead acid batteries, would provide a way to mitigate this issue [22].

Essentially, from the iron electrode point of view, the main process taking place during its charging process is the reduction of ferrous ion (Fe^{2+}) to metallic iron (Fe^0); in the same manner, the oxidation of metallic iron to ferrous ions take place during the discharging process of the iron electrode. Eq. (1) illustrates the charging and discharging (forward and backward reactions respectively) processes of an iron electrode under alkaline conditions [14,23,24].



It is well known, however, that during the charging of an iron electrode (under alkaline conditions), water is decomposed to yield hydrogen. Therefore, part of the energy, that was originally intended to be stored in the battery, is finally wasted in the parasitic evolution of hydrogen. In other words, hydrogen evolution accounts for a drastic reduction in the overall performance of the battery, as indicated by Eq. (2) [24].



Many attempts have been made in order to mitigate or even prevent the evolution of hydrogen during the charging of the iron electrode. The most promising strategies rely in the modification of the iron electrode formulation, by either nano-structuring the electrode or by the addition of elements (such

as sulphur or bismuth) that are capable to increase the overpotential for hydrogen evolution [25–27]. As a consequence, different electrode formulation additives have been utilised to achieved that aim, including bismuth [28], bismuth sulphide [26], carbonaceous materials [29–31], iron oxide [32,33], etc. Undoubtedly, the development of sulphur based iron electrode formulations is one of the most promising alternatives [25]. Moreover, the performance of the NiFe cells can also be further improved by optimising the electrolyte composition; in fact, different electrolyte additives such as wetting agents [34], long chain thiols [35], organic acids [36], among others have been investigated. Our experimental results confirm the addition of soluble sulphur species will enhance the performance of the NiFe battery [37,38].

In the quest for a highly efficient NiFe battery, different materials and manufacturing strategies have been used; in fact, nickel-iron cells reaching nearly 800 mAh/g have been reported [27,39], unfortunately these batteries require costly reactants and nano-structuring techniques. These aspects would certainly influence the final price of the battery thus produced [27,39].

Without pretending to give a full introduction on experimental design or multivariate statistics, we would like to underscore the importance of using a framework that allows us to deal with multidimensional problems, especially when large variability across experiments is found or at least suspected. Basically, experimental design will provide the best evidence that factors would account for your response variables with certain degree of certainty (the so-called α level).

Under the light of our previous arguments, we have decided to investigate and improve aqueous nickel-iron cells as cost effective solutions to store grid-scale amounts of energy. Broadly speaking, we have been using experimental design and multivariate analysis to facilitate our research [26,28,40]. In this manuscript, a 3×4 full factorial design has been used to investigate the incidence of both lithium hydroxide and potassium sulphide in the electrolyte as a means to increase the hydrogen energy barrier (thus preventing hydrogen evolution from the decomposition of the electrolyte). In addition, we have used FeS/Fe based electrodes as anodes, commercial nickel electrodes as cathodes, and concentrated solutions of potassium hydroxide as the electrolyte system. The production details of the electrodes can be found elsewhere [26,37].

Experimental

Iron based electrodes were produced by coating strips of nickel foam with an Fe/FeS active paste which consists of varying amounts of electroactive material (with this term we mean iron) with a mixture of iron sulphide and PTFE (acting as a binder). The chemicals and materials used to develop our electrode formulations were of the following specifications.

Iron powder (purity 99.5%, $<10\ \mu\text{m}$) from Alfa Aesar
 Iron sulphide (purity 99.5%) from Sigma Aldrich
 PTFE (Teflon 30-N, 59.95% solids) from Alfa Aesar
 Nickel foam (purity 99.0%, density $350\ \text{g/m}^2$) from Sigma Aldrich

Essentially, strips of nickel foam (10 mm × 40 mm × 1.8 mm) were coated and then vacuum dried for at least 5 h until a constant amount of electroactive material (iron) was loaded onto the electrode; this coating process was repeated until approximately 0.2–0.25 g of iron powder were loaded on an area of approximately 1 cm². When the process was finished, the electrodes were vacuum dried for another day to ensure consistency. Iron electrodes of the following characteristics were thus produced: 11% FeS + 6%PTFE + 83%Fe.

In our previous investigations regarding the role of selected electrode additives (such as potassium sulphide, bismuth sulphide, elemental bismuth and iron sulphide) in the performance of the iron electrode [26,28], we have found that although, the soluble bisulphite anion is responsible for an enhancement of cell performance, potassium sulphide only marginally improves the overall efficiency of the NiFe cell. This experimental observation seems rather counterintuitive, of course, however, we now believe the amounts of potassium sulphide that we used then, are in fact very low to be significant, and it should be investigated at larger compositions. This can only be achieved by using it as an electrolyte component. Moreover, the role of lithium hydroxide as an electrolyte additive is not fully understood, it has been suggested its presence would enhance the working life of the battery, and therefore, it is usually encounter with most NiFe electrolyte systems at a concentration close to 0.1 M. However, not much has been said about its role in enhancing the performance of the battery. With this in mind, electrolyte systems for NiFe cells based on lithium hydroxide and potassium sulphide were tested. The specifications of the chemicals and materials used to produce the electrolyte solutions were as follows: Potassium hydroxide (purity ≥ 85.0%, pellets) from Sigma Aldrich. Potassium sulphide (purity ≥ 99.5%) from Sigma Aldrich. Lithium hydroxide (purity ≥ 98.0%) from Sigma Aldrich. In house deionized water was produced by using an Elix 10-Milli-Q Plus water purification system (Millipore, Eschborn, Germany). In order to investigate the effect of additives on cell performance, electrolyte systems based on Table 1 were used.

As electrolyte systems for NiFe cells require potassium hydroxide to be in vast excess relative to other constituents, we decided to keep its concentration constant and explore the effect of the other components in the electrolyte system. Essentially, we have kept the composition of potassium hydroxide at a constant value of approximately 5.1 M. Based on the constancy of KOH and on Table 1, a 3 × 4 full factorial design was proposed to investigate the combined effect of potassium sulphide and lithium hydroxide as electrolyte components for NiFe cells. The final definition of factors and levels for this experiment is shown in Table 2.

Table 1 – Experimental conditions (compositions on a PTFE-free basis).

Additive	Range of concentrations (M)	
	Low	High
LiOH	0	0.3
K ₂ S	0.0	0.6

Table 2 – Experimental definitions of factors and levels.

Factors and levels		LiOH (0.0–0.3 M)		
		L1	L2	L3
K ₂ S (0.0–0.6 M)	L1	(0.0, 0.0)	(0.0, 0.15)	(0.0, 0.3)
	L2	(0.2, 0.0)	(0.2, 0.15)	(0.2, 0.3)
	L3	(0.4, 0.0)	(0.4, 0.15)	(0.4, 0.3)
	L4	(0.6, 0.0)	(0.6, 0.15)	(0.6, 0.3)

Table 3 – Experimental design matrix and results for the 50th cycle.

Cell	K ₂ S (M)	LiOH (M)	u_Q	η_Q
A	0.0	0.0	16.7 ± 0.8	23.5 ± 2.2
B	0.0	0.15	14.8 ± 0.5	24.2 ± 1.6
C	0.0	0.3	15.1 ± 1.2	25.2 ± 1.8
D	0.2	0.0	14.5 ± 0.9	26.5 ± 2.0
E	0.2	0.15	14.6 ± 0.4	26.5 ± 2.2
F	0.2	0.3	16.4 ± 1.1	26.8 ± 2.6
G	0.4	0.0	14.1 ± 0.7	30.5 ± 2.7
H	0.4	0.15	13.8 ± 1.5	33.2 ± 2.7
I	0.4	0.3	15.7 ± 1.4	30.9 ± 3.1
J	0.6	0.0	14.2 ± 1.0	30.5 ± 2.4
K	0.6	0.15	18.4 ± 3.1	33.1 ± 2.8
L	0.6	0.3	15.6 ± 1.6	31.3 ± 3.0

The electrolyte formulations appearing in Table 2 were tested on a three electrode cell. In-house produced bismuth sulphide based iron electrodes were tested in a three-electrode cell. Nickel electrodes (obtained from a commercial battery) were used as the positive terminal of the cell. All potentials were measured against a mercury/mercury oxide reference electrode ($E^0_{\text{Hg}/\text{HgO}} = 0.098 \text{ V vs. NHE}$).

A 64 channel Arbin SCTS was used to conduct experiments of charge and discharge under galvanostatic conditions at room temperature until the steady state was reached. Cells were cycled from 0.6 to 1.4 V vs. Hg/HgO at a C/5 rate. Formation and stabilization of the electrodes were found to be complete by the 50th cycle of charge and discharge [26,28]. Fig. 1 provides a sketch of the cell test configuration.

Cyclic voltammetry and electrochemical impedance spectroscopy (EIS) measurements were conducted on an 8-channel Solartron 1470E/1455A potentiostat/galvanostat with

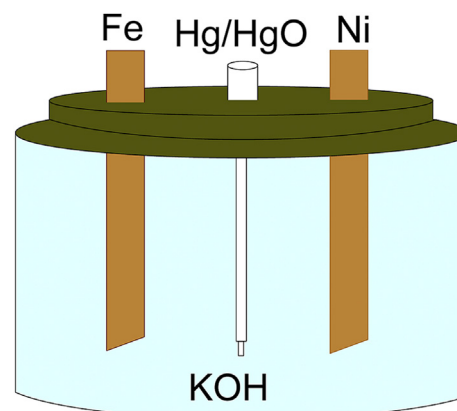


Fig. 1 – Test cell configuration.

frequency response analysers. The electrochemical measurements were made using a conventional three-electrode glass cell at room temperature (25 °C). The working electrode was a polished iron disk electrode (EIS measurements), this electrode was coated with an iron-rich paste of the same composition than our in-house made iron electrodes to conduct CV experiments; the reference electrode was a mercury/mercury oxide (Hg/HgO) electrode; finally, a platinum wire was used as a counter electrode. CV experiments were performed between 0 and -1.2 V (vs. Hg/HgO) at a sweep rate of 500 mV s^{-1} . EIS impedance spectra were recorded as a function of electrode potential using a 10 mV perturbation over the frequency range from 100 kHz to 10 mHz .

ATR-FTIR spectroscopy was used to characterise the surface chemistry aspects of iron electrodes by using a Bruker Alpha FTIR spectrometer with a diamond crystal that permits operating in the range of energies from between 400 and 4000 cm^{-1} .

Phase constitution was undertaken by XRD on a Bruker D2-Phaser, with Cu-K α 1 radiation ($\lambda = 1.5406 \text{ nm}$). The 2θ angular region from between 15° and 85° was scanned at a constant rate (1 min^{-1}), with a step size of 0.1° and increment of 0.02° ; finally, the detector was set to 0.27 V of the lower detection limit.

Results and discussion

It has been recognized that any NiFe cell requires a relatively long conditioning period (in the order of 30 cycles of charge and discharge) before it reaches the steady state. Figs. 2–4 confirm this observation, and shows that in general, the performance of any battery increases from nearly zero (in the early cycles of charge–discharge) up to more than 60%.

In general terms, any NiFe battery requires a conditioning period before developing its full potential. It was proposed that this is because the electrode requires to achieve a favourable configuration that is dependent not only upon its

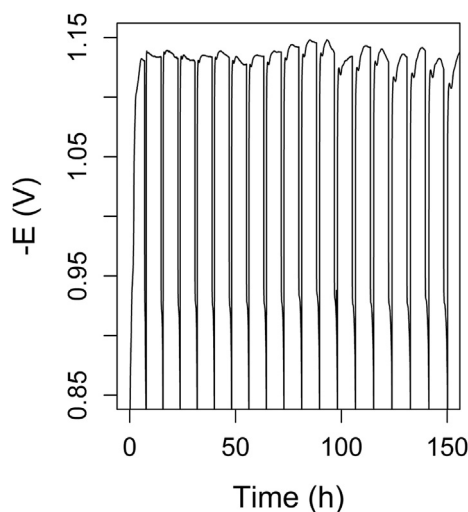


Fig. 2 – Charge and discharge profile for a NiFe cell using electrolyte system F (Table 3) versus mercury/mercury oxide (Hg/HgO) reference electrode.

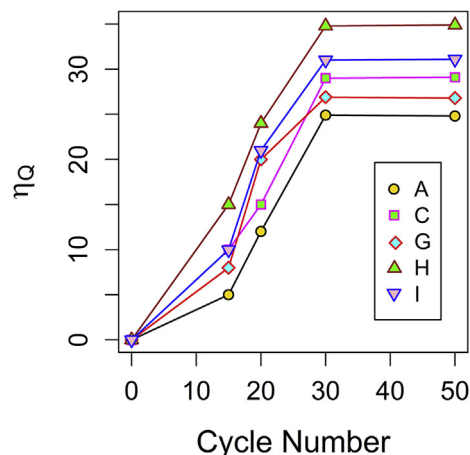


Fig. 3 – Coulombic efficiency versus cycle number for selected electrolyte systems (please refer to Table 3).

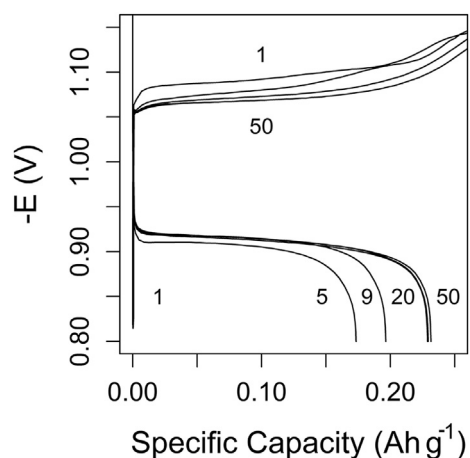


Fig. 4 – Selected charge and discharge curves for electrolyte system H (from Table 3) versus mercury/mercury oxide (Hg/HgO) reference electrode. The upper curves represent the charging of the electrode (cycles 1, 5, 9, 20, 50).

composition but on the electrolyte system as well. Once the conditioning period was completed, the battery reaches its full potential and will exhibit a very long cycle life without significant reduction in performance.

Fig. 4 confirms the existence of the aforementioned conditioning period for selected cells for different electrolyte systems. It is important to highlight the fact that although, the electrolyte systems are different and the performance of the cells are different, all cells tend to reach the steady state after 30 cycles, however the electrolyte system.

Table 3 lists experimental values of coulombic efficiency and utilization of electroactive material for our in-house made electrodes in different electrolyte systems. As can be seen, the data exhibits large variability so a relatively large number of replicates (12 in this case) were required to increase the statistical force of the analysis. With this in mind, any sample whose coulombic efficiency or utilization of electroactive material lays more than two standard deviations from the mean was rejected.

Table 3 reveals large variability across electrode formulations. Similar behaviour has been noted in our previous investigations [26,28,40], it is our belief this problem could be ascribed to inconsistencies (such as mixing or homogenizing mixtures of metallic powders) during the electrode manufacturing process.

In order to determine the relationship between the factors and responses (coulombic efficiency, utilization of electroactive material and compositions of lithium hydroxide and potassium sulphide), different polynomial functions, as the one represented by Eq. (3) were used.

$$\psi = a_0 + a_1 Y_K + a_2 Y_K^2 + a_3 Y_L + a_4 Y_L^2 + a_5 Y_K Y_L \quad (3)$$

where ψ represents any of the response variables, either coulombic efficiency (η_Q) or utilization of electroactive material (U_Q); the a 's represent the expansion coefficients (where any positive sign in front of each coefficient indicates a synergistic effect; likewise, any negative sign indicates an antagonistic effect.), the Y terms represent the composition of each component (in mol/L) and the subscripts K and L denote potassium sulphide and lithium hydroxide respectively.

Even though the degree of association between variables is relatively low, due to the significance of model (large F -statistic values), we could conclude that both lithium hydroxide and potassium sulphide enhance cell performance for intermediate concentrations of both additives. Although, we haven't included any test for normality, our results indicate that at the level of significance $\alpha = 0.05$, there is no evidence against normality, nor we found reasons to suspect heteroscedasticity; and in fact, as shown in Table 4, logarithmic transformations, which provide a means to deal with such situations, did not significantly improve model fit.

As indicated by Table 3 and Eq. (4), coulombic efficiency can be explained as a function of electrolyte composition; however, due to the large scattering in our data, Fig. 5 reveals a visual inspection of results would hardly help to identify the nature of the association between battery performance and electrolyte composition. In situations like this, dimensionality reduction would help reveal finding the true nature of the association between response variable and factors.

Fig. 6 illustrates the use of a multi-scattering diagram, in helping visualize how the response variable, coulombic efficiency, is affected by the concentration potassium sulphide at different levels of lithium hydroxide.

The bottom left part of Fig. 6 shows how at low LiOH concentrations, coulombic efficiency increases with the presence of potassium sulphide until 0.4 M where it reaches a plateau. This behaviour holds at intermediate (low right part of the diagram) and at high (upper part of the diagram) concentrations of LiOH. It is therefore, not surprising that a second order

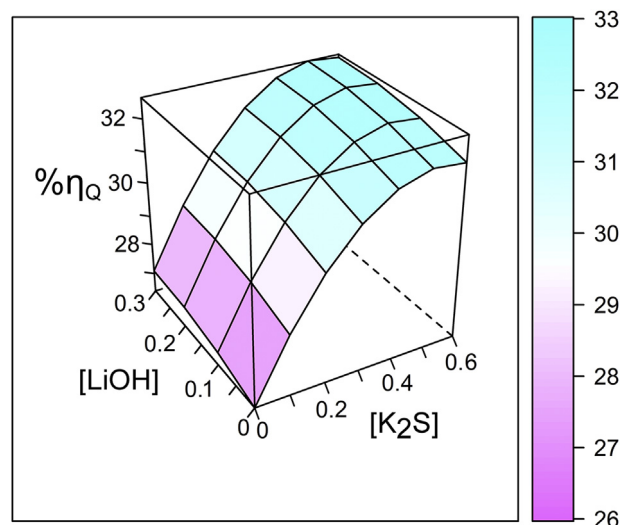


Fig. 5 – Second order three dimensional representation of coulombic efficiency as a function of electrolyte composition (in mol/L).

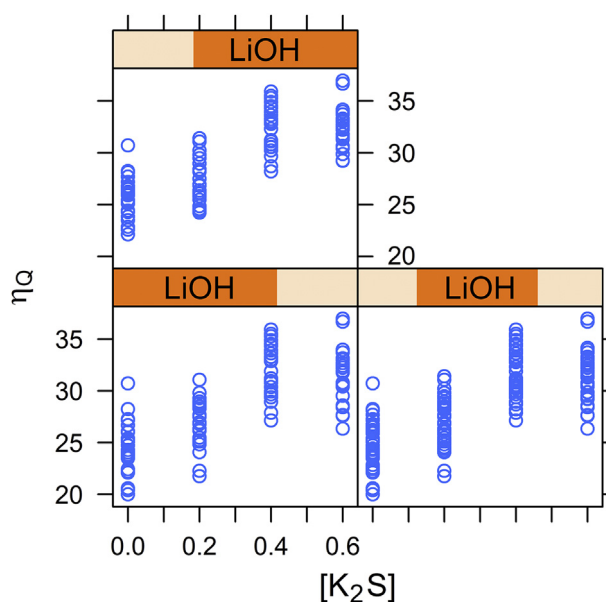


Fig. 6 – Incidence of K_2S and $LiOH$ on coulombic efficiency. Concentrations in mol/L.

model would make more sense to represent our data than a linear model.

After using the generalized linear regression model the following relationship between the response variable (coulombic efficiency) and the factors (composition of potassium sulphide and lithium hydroxide), the following relationship was found:

$$\eta_Q = 24.27 + 12.43Y_K + 5.75Y_L - 1.59Y_K Y_L \quad (4)$$

It is important to highlight that we have found no evidence that any of the least squares regression assumptions are violated, so Eq. (4) holds. The regression analysis reveals that despite a relatively low multiple correlation coefficient ($r^2 = 0.5677$), the model represented by Eq. (4) is significant (F

Table 4 – Regression parameters for selected forms of Eq. (4).

Model/parameter	η_Q		u_Q	
	R^2	F-statistic	R^2	F-statistic
Linear	0.57	92.55	0.015	1.072
Quadratic	0.64	48.89	0.12	6.36
Logarithmic	0.57	93.47	0.017	1.213

value of 61.3), and all terms but the mixed $Y_K Y_L$ from the model are significant. We have repeated the calculation by considering second order models and even standard transformations (square root and logarithmic) but as shown in Table 4, the improvement was at best nominal.

By using the fundamental theory of calculus and Eq. (4) it is possible to demonstrate that coulombic efficiency renders increased performance at the boundaries of the concentration space, this is 0.6 M K_2S and 0.3 M $LiOH$. However, when using 0.4 M K_2S and 0.15 M $LiOH$ the performance of the battery seems to be indistinguishable that when using the optimal formulation. Electrolyte systems containing 0.4 M K_2S and 0.15 M $LiOH$ (formulation H) rendered coulombic efficiencies in the order of 35%. A close look at Eq. (4) reveals a very large expansion coefficient of potassium sulphide, almost two times larger than its corresponding lithium hydroxide counterpart; this would indicate the presence of potassium sulphide increases cell performance to a much larger extent than the presence of lithium hydroxide.

Utilization of electroactive material was explained by the composition factors (K_2S and $LiOH$ content). Fig. 7 provides a two dimensional representation of the data and Eq. (5) shows the dependency between factors on response variable.

$$u_Q = 16.27 - 4.25Y_K - 5.75Y_L + 26.35Y_K Y_L \quad (5)$$

In terms of utilization of electroactive material, the situation is a bit less evident. Neither of the models are capable to explain the observed experimental data. The correlation was marginally improved by using standard transformations, for this reason the results are not shown. Therefore, the best way to represent the utilization of electroactive material is the mean of the data set (16.27), which is given by the independent term from Eq. (5). Basically, our experimental results show that Eq. (5) is of limited use in describing the incidence of electrolyte additives on the utilization of electroactive

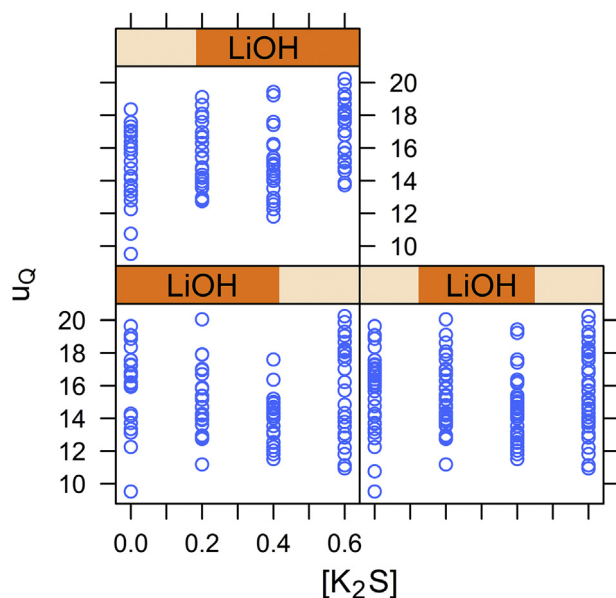


Fig. 7 – Incidence of K_2S and $LiOH$ on utilization of electroactive material. Concentrations in mol/L.

material. In general, the regression coefficient and the F-statistic are both very low (refer to Table 4).

Eq. (5) reveals similar expansion coefficients for potassium sulphide and lithium hydroxide; therefore, it follows that in this case, both additives seem to be equally relevant. However, we have seen that the utilization of electroactive material is not truly mirrored by any polynomial expression of the form given by Eq. (3) and moreover, it is the mean the parameter that best reflects the sample. Therefore, it necessarily follows that we lack evidence to correlate the use of either potassium sulphide and lithium hydroxide with the utilization of electroactive material, under the experimental conditions considered here.

Although, we have used a relatively large number of replicates and the two standard deviation criteria for sample rejection, reproducibility still remains as a major concern. As the methodology for producing electrolyte systems is relatively simple, the authors believe the origin of the variability can be traced to the production of the anodes. Reasons for such variability have been already identified [26,28,40].

By utilizing our in-house made iron based electrodes and an electrolyte composed of 5.1 M KOH + 0.4 M K_2S + 0.15 M $LiOH$, we have produced NiFe cells rendering coulombic efficiencies in the order of 35%, which is not great, so the next question is whether the evolution of hydrogen can be further reduced. In this part of the research, electrode formulations will be developed by utilizing our previously optimized electrolyte system and by using a similar methodology to the one used with our previous research, the details can be found elsewhere and the reader is invited to explore those resources [26,40].

Fig. 8 suggests there are two main regions (FeS dependent) that render different battery performance: the first one with relatively low coulombic efficiencies (~35%) and large capacities (~230 mA/g), the second region is characterized for rendering cells with very low capacities (~60 mA/g) but very high coulombic efficiency values (~95%). From these experimental results, we can conclude it is possible to reduce the evolution of hydrogen from iron based electrodes, but this would come to a price: lower capacity.

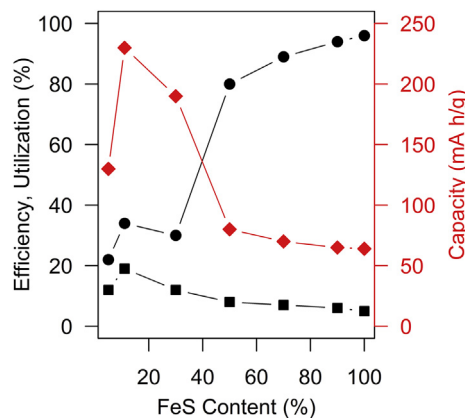


Fig. 8 – Combined performance plot for NiFe cells by using electrolyte system H (Table 3). Key: circles coulombic efficiency, squares utilization of electroactive material, diamonds capacity.

Fig. 9 shows a representative 600 to 5000 cm^{-1} ATR-FTIR spectra for one of our electrodes after 50 cycles of charge and discharge. Basically, the spectra include a signal near 660 cm^{-1} corresponding to either Fe–S or Fe–O stretching; a weak signal appearing near 930 cm^{-1} corresponding to Fe–OH stretching; a very broad peak appearing at 3300 cm^{-1} corresponding to OH stretching was also found; however, this last peak could be due to some adsorbed water molecules or some remaining potassium or lithium hydroxide (coming from the electrolyte).

As described in the experimental part, iron electrodes were produced with 11% FeS + 6%PTFE + 83%Fe, the XRD of the electrodes before and after the experiments of charge and discharge, exhibit no meaningful differences. We believe that this is because the reaction between metallic iron (the electroactive material of the electrode) and the soluble bisulphite anion is not favoured. Furthermore, the utilization of the electroactive material is relatively low, so it necessarily follows that only a small amount of Fe/FeS of the total is actually active; therefore, the XRD trace is fully dominated by iron and iron oxide signals.

We have reported the use of low concentrations of potassium sulphide as an electrode additive only marginally effects the overall performance of NiFe cells [26,28]. However, the use of potassium sulphide at large concentrations seems to enhance the overall performance of the battery. This new finding persuades us to believe that at sufficiently large concentrations, the presence of the soluble bisulfide anion (HS^-) becomes important to explain the coulombic efficiency of the cell.

Fig. 10 shows a typical XRD trace of one of our electrodes after 50 cycles of charge and discharge. This figure confirms the presence of α -Fe but we haven't found any evidence of other polymorphs of iron (neither β -Fe nor γ -Fe), nor we have found compelling evidence of the presence of the spinel Fe_3O_4 [41]; however, we had found a weak signal appearing approximately at $2\theta = 24^\circ$ which would correspond to either α - Fe_2O_3 or $\text{Fe}(\text{OH})_2$; note the transformation of Fe_3O_4 into α - Fe_2O_3 have been reported to be possible [42].

From the XRD analysis, it follows that all observed sulphur related peaks belong to diffraction reflections of hexagonal

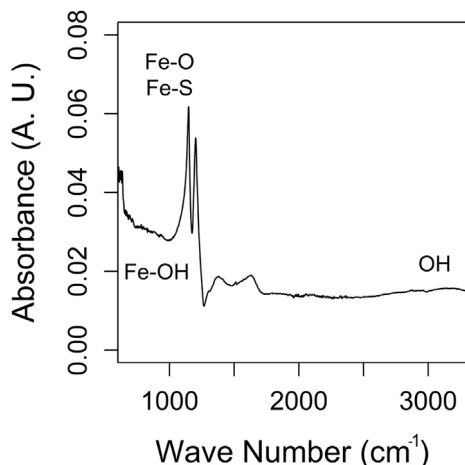


Fig. 9 – ATR-FTIR spectra of an iron electrode using electrolyte system H (Table 3).

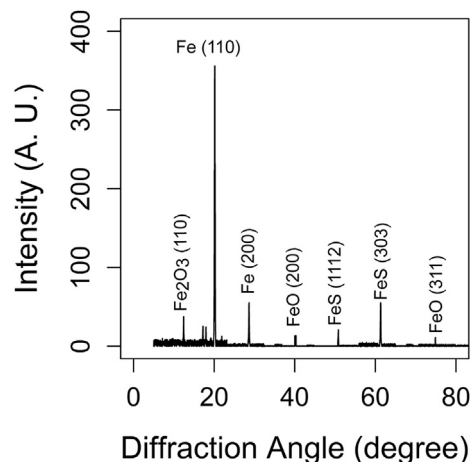


Fig. 10 – XRD of an iron electrode after being cycled 50 times using electrolyte system H (Table 3).

iron sulphide ($\text{P6}_3/\text{mmc}$, space group 194). No XRD evidence of other forms of sulphur was found. Basically, no compelling evidence of any form of iron oxyhydroxide was found in our samples; this can be rationalised by recognising that under alkaline conditions; Fe(III) could transform into from β - FeOOH and then to α - Fe_2O_3 , and moreover, either goethite (α - FeOOH) or akaganeite (β - FeOOH) can transform into α - Fe_2O_3 [43], which means that the signal appearing at $2\theta = 24^\circ$ could very well be due to either of those species after transforming into α - Fe_2O_3 . However, this very same signal could be related with $\text{Fe}(\text{OH})_2$, which can be further oxidised into either magnetite (cubic spinel Fe_3O_4) [44], goethite, akaganeite or lepidocrocite (γ - FeOOH) [45], to finally transform into α - Fe_2O_3 . Magnetite can also undergo transformation into γ - Fe_2O_3 and then into α - Fe_2O_3 [46].

Although, our results confirm that battery performance is enhanced by the presence of relatively large amounts of potassium sulphide in the electrolyte, the functional Fe–S groups detected within the electrodes were not meaningfully affected by its presence. This is, no direct evidence of reaction between potassium sulphide and the electrodes was found.

In conclusion, under our experimental conditions, we found no evidence of any reaction between potassium sulphide and either iron sulphide or metallic iron. However, the absence of evidence it is not necessarily evidence of absence, therefore, we can only conclude that our results are inconclusive and more research is still needed.

In order to investigate the electrochemical properties of the cell, cyclic voltammetry experiments were conducted under conditions that maximise coulombic efficiency; this is 5.1 M KOH + 0.4 M K_2S + 0.3 M LiOH. As shown in Fig. 11, three distinctive peaks that can be easily noted:

- Ox_1 : would correspond to the oxidation of Fe(0) to Fe(II) as represented by Eq. (6).
- Ox_2 : would correspond to the formation of δ - FeOOH [47], and/or Fe_3O_4 can also proceed as suggested by Eq. (7) and Eq. (8).
- Red_1 : would correspond to the reduction of Fe(II) to Fe(0) as represented by Eq. (6).

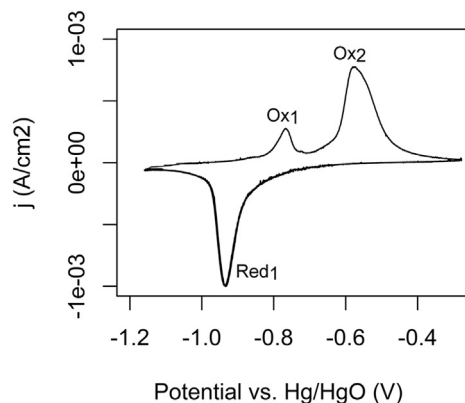
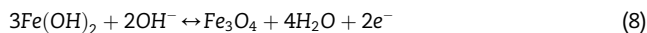
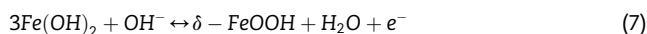


Fig. 11 – Cyclic voltammetry of an iron electrode (80% FeS + 6%PTFE + 14%Fe) after being cycled 50 times using electrolyte system H (Table 3), at a scan rate of 500 mV s⁻¹.

The electrochemical processes represented by Eq. (6) to Eq. (9) have been reported whenever iron is exposed under strong alkaline conditions (either KOH or NaOH) [48].



It is supposed that sulphur containing species such as iron sulphide could improve the performance of a NiFe cell by controlling the corrosion state of the iron electrode [49–51], unfortunately, the detailed mechanism is not fully understood [52]. Our experimental evidence supports the idea that the use of potassium sulphide, as an electrolyte additive, does enhance the overall performance of the battery.

It is known that the entering of hydrogen into iron metals and alloys is promoted by sulphur containing compounds such as HS⁻, S²⁻ and H₂S [53,54]. The passive film on iron would consist many different forms of iron such as magnetite, maghemite, among others [55,56]. The aforementioned layer would be formed through the participation of anionic octahedrally coordinated iron oxyhydroxide complexes that might be present on the surface of the electrode [57]. Hydrogen, as a reducing agent, would certainly have a real incidence in the reduction of the different forms of iron within the electrode. From these ideas, it necessarily follows that the passivation of the iron electrode can be controlled by its hydrogen content.

Fig. 3 confirms the existence of a conditioning period, where electrode performance increases with the cycling number, until steady state conditions are reached. We have observed, during this conditioning period, that the electrodes fall apart. It has been reported that hydrogen evolution and ingress into iron is strongly enhanced by renewal of the metal surface [58], it is our belief, therefore, that during the conditioning period new surface area is generated with the breaking up of the electrode, until steady state is reached.

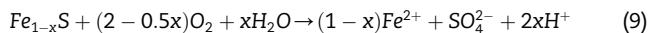
We believe that a synergistic effect between the generation of electroactive surface area, hydrogen ingress into the electrode and its composition are essential to achieve an

understanding of the reactivity of the iron electrode. These ideas are supported in part by observations that have been made during the hydrogen evolution reaction under alkaline conditions [59], and our experimental findings [37,38,40].

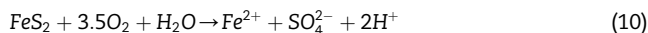
Fig. 12 shows a Nyquist plot obtained by utilizing a bare iron disk electrode in selected electrolyte systems. EIS measurements suggest the formation of adsorbed layers of sulphur containing species.

A simple electrical equivalent circuit consisting in a series arrangement of the Ohmic resistance (R_Ω) and a parallel arrangement of the capacitance associated with the capacitance of the double layer (C_{dl}) and the charge transfer resistance for hydrogen evolution (R_{ct}). This model has been validated for similar soluble sulphur containing species at the iron/electrolyte interface and similar results have been reported [24,35]. Our experimental findings confirm that the presence of the soluble bisulphite anion (HS⁻) lowers the double layer capacitance and increases the charge transfer resistance for hydrogen evolution.

By considering the formation of Na–S species and under the light of our results, we have proposed that during the charge and discharge process of the electrode. In the presence of oxygen, sulphur containing species (such as pyrites) can be oxidised into ferrous ions according to the following reaction.



In the presence of oxygen, pyrites are oxidised according to Eq. (10).



The high alkaline medium, close to 28.5% KOH, will displace Eq. (10) to the right (Le Châtelier's principle), thus rendering the ferrous ions the battery requires to properly functioning.

In the presence of oxygen, FeS would react rendering ferrous ions and sulphate ions.



Any FeS₂ present in the electrode might be reduced into elemental iron.

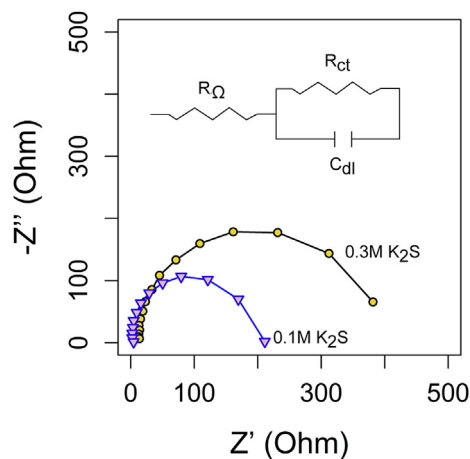


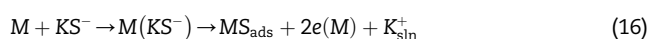
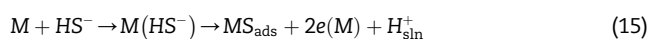
Fig. 12 – Impedance data for iron disc electrode in strong KOH.



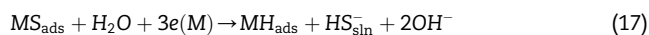
Eq. (9) to Eq. (14) would explain the generation of iron from FeS/FeS₂ in the electrode.

It has been proposed that sulphur containing species such as iron sulphide could improve the performance of the iron electrode by controlling its corrosion state [49–51], however, the detailed mechanism is not fully understood [52].

It has also been reported that hydrogen can enter into transition metals such as iron, and that this process is favoured by presence of sulphur containing compounds [53,54]. Moreover, it is well known that species such as HS⁻, S²⁻ and H₂S are common promoters of hydrogen ingress into iron [54]. We have proposed that soluble sulphur species (such as HS⁻ or KS⁻) from the electrolyte could interact with the electrode (electrosorptive process) [37,38].



In this way, the formation of MS_{ads} will promote the ingress of hydrogen into the electrode as suggested by Eq. (17).



As indicated by Eq. (17), the ingress of hydrogen into the electrode will promote the release of HS⁻ and OH⁻, thus regenerating both electrode and electrolyte [38].

Therefore, it necessarily follows that iron electrodes produced at large concentrations of iron sulphide should exhibit, and indeed they do, better charge and discharge properties than their low concentration counterparts.

It has been reported that hydrogen evolution and ingress into iron is strongly enhanced by renewal of the metal surface [58]. Figs. 2 and 3 confirm that the performance of the Fe/FeS electrodes increases with the cycling number, until steady state conditions are reached.

Finally, the authors believe that the reactivity of the FeS electrode can be explained in terms of the very same iron active species that can be found in conventional Fe based anodes for NiFe cells. The authors felt the degradation of the electrode that might occur during the conditioning period is key to understand the reactivity of the Fe/FeS electrode. These ideas are supported in part by observations that have been made during the hydrogen evolution reaction under alkaline conditions [59].

Conclusions

By pursuing the development of cost effective energy storage solutions, we have identified two main electrode formulation regions (FeS dependent). The first region is characterized for electrodes utilizing small amounts of iron sulphide and rendering relatively low coulombic efficiencies (~35%) and large capacities (~230 mA/g). Utilizing larger amounts of iron

sulphide, the second region is characterized for rendering cells with very low capacities (~60 mA/g) but very high coulombic efficiency values (~95%). From these experimental observations, it follows that it is possible to increase coulombic efficiency by preventing electrolyte decomposition during the charging of iron based electrodes, but this would come to a price: lower capacity.

It was found that potassium sulphide has a real incidence in the response variable; this is, under our experimental conditions, the addition of potassium sulphide increases coulombic efficiency of our NiFe cells.

The evidence gathered during this research project, supports the idea that the high concentrations of the soluble bisulfide anion (HS⁻) do improve the overall coulombic efficiency of our in-house made NiFe cells.

Our experimental findings would suggest there is no such a thing as a strong linear association between the composition of the electrolyte and the utilization of electroactive material. In fact, at low concentrations of potassium sulphide, the utilization of electroactive material marginally decreases with increasing the lithium hydroxide content. Conversely, at intermediate and high concentrations of potassium sulphide, the utilization of electroactive material slightly increases with increasing the electrolyte content of lithium hydroxide. In this case, it was not possible to find a function that correlates well the response variable and factors in a better way than the mean.

The data gathered during this project is subject to large variability; therefore, aiming to increase the statistical force of the analysis, we had used a relatively large number of replicates (12 in total) and used the two standard deviation criteria for rejection.

Multi-scattering diagrams provide a means to visualize the incidence of two variables on a response factor. In this case, we show the usefulness of these diagrams in the analysis of data gathered during the charge and discharge of relatively large numbers of nickel iron cells.

EIS results suggest the soluble bisulphite anion (HS⁻) lowers the double layer capacitance and increases the charge transfer resistance for hydrogen evolution.

Finally, our experimental findings would suggest that at the level of confidence $\alpha = 0.05$, potassium sulphide, as electrolyte additive, does enhance the performance of the battery. Although less clear, a similar conclusion can be drawn for lithium hydroxide.

Acknowledgements

The authors would like to acknowledge the U.K. Engineering and Physical Sciences Research Council for supporting this work (EP/K000292/1; SPECIFIC Tranche 1: Buildings as Power Stations).

REFERENCES

- [1] Armand M, Tarascon JM. Building better batteries. *Nature* 2008;451:652–7.

- [2] Hedegaard K, Meibom P. Wind power impacts and electricity storage – a time scale perspective. *Renew Energy* 2012;37:318–24.
- [3] Chen H, Cong TN, Yang W, Tan C, Li Y, Ding Y. Progress in electrical energy storage system: a critical review. *Prog Nat Sci* 2009;19:291–312.
- [4] Jacob A. Wind energy – the fuel of the future. *Reinf Plast* 2001;45(Suppl. 1):10–3.
- [5] Tapiador FJ. Assessment of renewable energy potential through satellite data and numerical models. *Energy & Environ Sci* 2009;2:1142–61.
- [6] Rugolo J, Aziz MJ. Electricity storage for intermittent renewable sources. *Energy & Environ Sci* 2012;5:7151–60.
- [7] Barnhart CJ, Dale M, Brandt AR, Benson SM. The energetic implications of curtailing versus storing solar- and wind-generated electricity. *Energy & Environ Sci* 2013;6:2804–10.
- [8] Hart EK, Jacobson MZ. The carbon abatement potential of high penetration intermittent renewables. *Energy & Environ Sci* 2012;5:6592–601.
- [9] Jacobson MZ, Delucchi MA, Bazouin G, Bauer ZAF, Heavey CC, Fisher E, et al. 100% clean and renewable wind, water, and sunlight (WWS) all-sector energy roadmaps for the 50 United States. *Energy & Environ Sci* 2015;8:2093–117.
- [10] Baxter J, Bian Z, Chen G, Danielson D, Dresselhaus MS, Fedorov AG, et al. Nanoscale design to enable the revolution in renewable energy. *Energy & Environ Sci* 2009;2:559–88.
- [11] Schafer H, Sadaf S, Walder L, Kuepper K, Dinklage S, Wollschlager J, et al. Stainless steel made to rust: a robust water-splitting catalyst with benchmark characteristics. *Energy & Environ Sci* 2015;8:2685–97.
- [12] Gao P, Liu Y, Lv W, Zhang R, Liu W, Bu X, et al. Methanothermal reduction of mixtures of PbSO_4 and PbO_2 to synthesize ultrafine α - PbO powders for lead acid batteries. *J Power Sources* 2014;265:192–200.
- [13] Chaurey A, Deambi S. Battery storage for PV power systems: an overview. *Renew Energy* 1992;2:227–35.
- [14] Halpert G. Past developments and the future of nickel electrode cell technology. *J Power Sources* 1984;12:177–92.
- [15] Birch F. Density and composition of mantle and core. *J Geophys Res* 1964;69:4377–88.
- [16] Morard G, Siebert J, Andraut D, Guignot N, Garbarino G, Guyot F, et al. The Earth's core composition from high pressure density measurements of liquid iron alloys. *Earth Planet Sci Lett* 2013;373:169–78.
- [17] Oxley A, Barcza N. Hydro-pyro integration in the processing of nickel laterites. *Miner Eng* 2013;54:2–13.
- [18] Huang C-L, Vause J, Ma H-W, Li Y, Yu C-P. Substance flow analysis for nickel in mainland China in 2009. *J Clean Prod* 2014;84:450–8.
- [19] Braunschweig H, Cogswell P, Schwab K. Synthesis, structure and reactivity of complexes containing a transition metal–bismuth bond. *Coord Chem Rev* 2011;255:101–17.
- [20] Leonard NM, Wieland LC, Mohan RS. Applications of bismuth(III) compounds in organic synthesis. *Tetrahedron* 2002;58:8373–97.
- [21] Fray D. Metallurgy: iron production electrified. *Nature* 2013;497:324–5.
- [22] Gies E. Recycling: lazarus batteries. *Nature* 2015;526:S100–1.
- [23] Shukla AK, VenuGOPalan S, HariPrakash B. Nickel-based rechargeable batteries. *J Power Sources* 2001;100:125–48.
- [24] Yang B, Malkhandi S, Manohar AK, Surya Prakash GK, Narayanan SR. Organo-sulfur molecules enable iron-based battery electrodes to meet the challenges of large-scale electrical energy storage. *Energy & Environ Sci* 2014;7:2753–63.
- [25] Manohar AK, Yang C, Malkhandi S, Yang B, Prakash GKS, Narayanan SR. Understanding the factors affecting the formation of carbonyl iron electrodes in rechargeable alkaline iron batteries. *J Electrochem Soc* 2012;159:A2148–55.
- [26] Gil Posada JO, Hall PJ. Multivariate investigation of parameters in the development and improvement of NiFe cells. *J Power Sources* 2014;262:263–9.
- [27] Wang H, Liang Y, Gong M, Li Y, Chang W, Mefford T, et al. An ultrafast nickel-iron battery from strongly coupled inorganic nanoparticle/nanocarbon hybrid materials. *Nat Commun* 2012;3.
- [28] Gil Posada JO, Hall PJ. Post-hoc comparisons among iron electrode formulations based on bismuth, bismuth sulphide, iron sulphide, and potassium sulphide under strong alkaline conditions. *J Power Sources* 2014;268:810–5.
- [29] Hang BT, Watanabe T, Egashira M, Watanabe I, Okada S, Yamaki J-i. The effect of additives on the electrochemical properties of Fe/C composite for Fe/air battery anode. *J power sources* 2006;155:461–9.
- [30] Rajan AS, Sampath S, Shukla AK. An in situ carbon-grafted alkaline iron electrode for iron-based accumulators. *Energy & Environ Sci* 2014;7:1110–6.
- [31] Jiang W, Liang F, Wang J, Su L, Wu Y, Wang L. Enhanced electrochemical performances of FeO_x -graphene nanocomposites as anode materials for alkaline nickel-iron batteries. *RSC Adv* 2014;4:15394–9.
- [32] HariPrakash B, Martha S, Hegde M, Shukla A. A sealed, starved-electrolyte nickel–iron battery. *J Appl Electrochem* 2005;35:27–32.
- [33] Hang BT, Yoon S-H, Okada S, Yamaki J-i. Effect of metal-sulfide additives on electrochemical properties of nano-sized Fe_2O_3 -loaded carbon for Fe/air battery anodes. *J Power Sources* 2007;168:522–32.
- [34] Manohar AK, Yang C, Malkhandi S, Prakash GKS, Narayanan SR. Enhancing the performance of the rechargeable iron electrode in alkaline batteries with bismuth oxide and iron sulfide additives. *J Electrochem Soc* 2013;160:A2078–84.
- [35] Malkhandi S, Yang B, Manohar AK, Prakash GKS, Narayanan SR. Self-assembled monolayers of n-alkanethiols suppress hydrogen evolution and increase the efficiency of rechargeable iron battery electrodes. *J Am Chem Soc* 2012;135:347–53.
- [36] Mackenzie Jr MJ, Salkind Alvin J. Gas depressor additives for iron electrodes. 1969.
- [37] Posada JOG, Hall PJ. The effect of electrolyte additives on the performance of iron based anodes for NiFe cells. *J Electrochem Soc* 2015;162:A2036–43.
- [38] Posada JOG, Hall PJ. Towards the development of safe and commercially viable nickel–iron batteries: improvements to Coulombic efficiency at high iron sulphide electrode formulations. *J Appl Electrochem* 2016:1–8.
- [39] Manohar AK, Malkhandi S, Yang B, Yang C, Prakash GKS, Narayanan SR. A high-performance rechargeable iron electrode for large-scale battery-based energy storage. *J Electrochem Soc* 2012;159:A1209–14.
- [40] Gil Posada JO, Hall PJ. Surface response investigation of parameters in the development of FeS based iron electrodes. *Sustain Energy Technol Assessments* 2015;11:194–7.
- [41] Mosivand S, Kazeminezhad I. Functionalization and characterization of electrocrystallized iron oxide nanoparticles in the presence of β -cyclodextrin. *CrystEngComm* 2016;18:417–26.
- [42] Sharma R, Agrawal VV, Srivastava AK, Govind, Nain L, Imran M, et al. Phase control of nanostructured iron oxide for application to biosensor. *J Mater Chem B* 2013;1:464–74.
- [43] Musić S, Czakó-Nagy I, Salaj-Obelić I, Ljubešić N. Formation of α - Fe_2O_3 particles in aqueous medium and their properties. *Mater Lett* 1997;32:301–5.

- [44] Kharisov BI, Rasika Dias HV, Kharissova OV, Manuel Jimenez-Perez V, Olvera Perez B, Munoz Flores B. Iron-containing nanomaterials: synthesis, properties, and environmental applications. *RSC Adv* 2012;2:9325–58.
- [45] Miyamoto Hiroki, Shinjo Teruya, Bando Yoshichika, Takada T. Mossbauer effect of Fe in Fe(OH)₂. *Bulletin of the institute for chemical research*, 45. Kyoto University; 1968. p. 333–41.
- [46] Zhao B, Wang Y, Guo H, Wang J, He Y, Jiao Z, et al. Iron oxide(III) nanoparticles fabricated by electron beam irradiation method. *Mater Pol* 2007;25:1143–8.
- [47] Rubim JC. In situ spectroelectrochemical study of the passivation of iron in alkaline solutions. *J Chem Soc Faraday Trans 1 Phys Chem Condens Phases* 1989;85:4247–58.
- [48] Mahmoudi L, Kissner R. Electrode reactions of iron oxide-hydroxide colloids. *Dalton Trans* 2014;43:15407–13.
- [49] Jayalakshmi M, Nathira Begum B, Chidambaram VR, Sabapathi R, Muralidharan VS. Role of activation on the performance of the iron negative electrode in nickel/iron cells. *J Power Sources* 1992;39:113–9.
- [50] Lyons MEG, Burke LD. Enhanced oxygen evolution at an activated iron electrode in alkaline-solution. *J Electroanal Chem* 1984;170:377–81.
- [51] Balasubramanian TS, Shukla AK. Effect of metal-sulfide additives on charge/discharge reactions of the alkaline iron electrode. *J Power Sources* 1993;41:99–105.
- [52] Diez-Perez I, Sanz F, Gorostiza P. Electronic barriers in the iron oxide film govern its passivity and redox behavior: effect of electrode potential and solution pH. *Electrochem Commun* 2006;8:1595–602.
- [53] Williams G, McMurray HN, Newman RC. Surface oxide reduction by hydrogen permeation through iron foil detected using a scanning Kelvin probe. *Electrochem Commun* 2013;27:144–7.
- [54] Flis-Kabulska I, Flis J, Zakroczymski T. Promotion of hydrogen entry into iron from NaOH solution by iron-oxygen species. *Electrochimica Acta* 2007;52:7158–65.
- [55] Shao HB, Wang JM, He WC, Zhang JQ, Cao CN. EIS analysis on the anodic dissolution kinetics of pure iron in a highly alkaline solution. *Electrochem Commun* 2005;7:1429–33.
- [56] Lyons MEG, Doyle RL, Brandon MP. Redox switching and oxygen evolution at oxidized metal and metal oxide electrodes: iron in base. *Phys Chem Chem Phys* 2011;13:21530–51.
- [57] Doyle RL, Lyons MEG. An electrochemical impedance study of the oxygen evolution reaction at hydrous iron oxide in base. *Phys Chem Chem Phys* 2013;15:5224–37.
- [58] Flis-Kabulska I. Transient hydrogen permeation through iron after potential jumps from cathodic to anodic polarisation in NaOH solution. *Electrochem Commun* 2009;11:54–6.
- [59] Solmaz R, Kardaş G. Electrochemical deposition and characterization of NiFe coatings as electrocatalytic materials for alkaline water electrolysis. *Electrochimica Acta* 2009;54:3726–34.